Replication of spinodally decomposed structures with structural coloration from scales of the longhorn beetle *Sphingnotus mirabilis*

2013 Bioinspir. Biomim. 8 045003

(http://iopscience.iop.org/1748-3190/8/4/045003)

Bioinspir. Biomim. **8** (2013) 045003 (6pp) doi:10.1088/1748-3182/8/4/045003

Replication of spinodally decomposed structures with structural coloration from scales of the longhorn beetle *Sphingnotus mirabilis*

Yafeng Zhang, Biqin Dong, Xiaohan Liu and Jian Zi

Department of Physics, Key Laboratory of Micro and Nano Photonic Structures (MOE), and Key Laboratory of Surface Physics, Fudan University, Shanghai 200433, People's Republic of China

E-mail: liuxh@fudan.edu.cn and jzi@fudan.edu.cn

Received 15 April 2013
Accepted for publication 3 July 2013
Published 21 November 2013
Online at stacks.iop.org/BB/8/045003

Abstract

Scales of the longhorn beetle *Sphingnotus mirabilis* possess a disordered bicontinuous macroporous structure that resembles a structure formed by a phase-separation process of spinodal decomposition. By using the scales as templates, SiO_2 and TiO_2 structures were successfully replicated. Structural and optical characterizations show that the fabricated oxide structures are spinodal decomposition structures with only short-range order and display non-iridescent structural colors.

(Some figures may appear in colour only in the online journal)

1. Introduction

Disordered bicontinuous macroporous structures such as those formed by a phase-separation process known as spinodal decomposition (SD) [1] have received considerable attention in recent years due to their unique structural features, offering important applications in catalysis, matter separation, energy generation and photonics [2–5]. SD structures can be formed in polymers, metal alloys, glasses and ceramics [6–9]. Interestingly, SD structures with a characteristic length comparable to visible wavelengths have unique optical properties such as unusual light scattering, non-iridescent structural coloration and the existence of isotropic photonic pseudo-gaps [10–12] due to their structural short-range order. It may even be possible to open up a complete photonic band gap by increasing the refractive index contrast of constituent materials [13–15]. Fabrications of such SD structures in the optical regime are, however, rather challenging.

In the biological world, photonic structures have been exploited to produce structural coloration since Cambrian time [16–23]. Revealed natural photonic structures are diverse and delicate such that they could serve as protocols for our artificial design and fabrication of novel photonic materials and devices [19, 24–30]. Structural colors have many interesting properties that differ from pigment colors such as high brightness and saturation. Ordered photonic structures that possess both short- and long-range order, e.g. thin films, multilayers, diffraction gratings and photonic-crystal structures [31–33], display iridescence, a phenomenon of color change with viewing angles. On the other hand, disordered photonic structures that possess only short-range order show non-iridescent structural colors [23, 34–38]. In particular, SD structures were revealed in bird feathers and insects [11, 36, 37], displaying interesting non-iridescent structural colors.

In this paper, by using the scales of the longhorn beetle *Sphingnotus mirabilis* as templates, we successfully replicated SiO_2 and TiO_2 SD structures with a sol–gel method. The fabricated oxide SD structures possess only short-range order and display vivid structural colors in the visible. The fabrication process is shown to be simple and cost-effective as well.

2. Materials and methods

2.1. Scale sample

The longhorn beetle *S. mirabilis* (Coleoptera) belongs to the family of Cerambycidae which can be found in Papua New

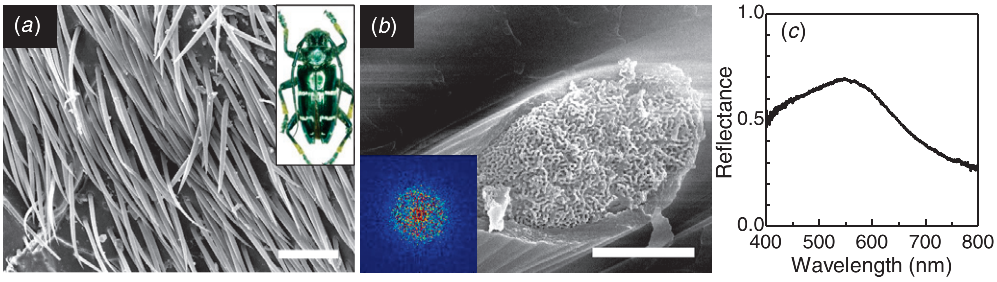

Figure 1. (*a*) SEM image of scales on the elytral surface of the longhorn beetle *S. mirabilis*. An image of the beetle is shown in the inset. (*b*) SEM cross-sectional image of a single scale. The inset shows the two-dimensional Fourier transform of the SEM transverse cross-sectional image of a scale. (*c*) Measured reflectance spectrum of a single scale. Scale bars: (*a*) 100 μm and (*b*) 5 μm.

Guinea. Specimens were bought from the Shanghai Natural Museum, Shanghai, China. Scales which served as templates for bio-replications were simply scraped off the elytra of the beetle by a razor blade.

2.2. Optical and structural characterization

Microscopic images of scales and fabricated oxide structures were recorded with an optical microscope (Leica DM6000 M). Microscopic optical spectra were measured by our home-built microspectrometer which consists of this microscope, a tungsten lamp as the light source, a 50× and NA 0.55 objective and an optical spectrometer (Ideaoptics PG2000pro EX), described in detail in [23]. The size of light beams impinging upon samples can be adjusted by a field diaphragm and a pinhole to 2–3 μm in order to enable the spectral analysis of a single scale. A diffuse reflectance standard (Ocean Optics) was used as reference for absolute reflectance measurements.

Microstructures of scales and fabricated oxide structures were characterized by scanning electron microscopy (SEM) (Philips XL30 FEG) which is equipped with energy dispersive x-ray spectroscopy (EDS) for composition analysis. In order to observe the inner structures of scales and fabricated structures, a slicer (Leica RM2255) or Ar ion etching was used for cutting or milling.

2.3. Replication technique

Techniques adopted for bio-replications include sol–gel, atomic layer deposition, physical vapor deposition and chemical vapor deposition. Among them, the sol–gel method has been frequently used to replicate various natural photonic structures such as beetle scales [25, 26], feather barbs [27] and butterfly wings [39]. The advantage of this method is simple and low-cost as well and thus can be adopted for mass production.

For SiO_2 replications, tetraethylorthosilicate, hydrochloric acid and ethanol were mixed as precursor. The stoichiometric proportion of the precursor was taken to be the same as that used in [27]. The mixture was then stirred with a magnetic stirring bar for 3 h to obtain a SiO_2 sol solution. Scales scraped off the elytra were placed between two conventional glass slides (about 75 mm × 25 mm in dimension and approximately 1 mm in thickness), adhered by two stripes of double sticky tape at the ends in order to form an air gap of about 10 μm in the middle. The glass slides were simply pretreated in ethanol, cleaned then by deionized water and finally dried in a dry oven. A small amount of prepared SiO_2 sol was then dropped through the air gap of the slides in order to allow a slow infiltration into the bio-templates via capillary effects. After the ethanol solvent was completely evaporated for more than 20 min, the slides with the scales were put in an oven and dried at 80 °C for 15 min. The above steps were repeated three or four times until the structural colors of the scales disappeared completely.

For TiO_2 replications, titanium tetrachloride (0.076 g), isopropyl titanate (0.209 mL) and ethanol (150 mL) were mixed and then stirred for 3 h. The other steps are basically similar to those for SiO_2 replications.

After the infiltration of the sol precursor and solidification of gel, two post-processing methods were used to remove the bio-templates, i.e. pyrolysis and acid-etching. For pyrolysis, samples were put in a muffle furnace at 550 °C for 300 min. For acid-etching, a mixture of HNO_3 and $HClO_4$ was used. Samples were immersed into the mixture at 130 °C for about 15 min. Both approaches can reliably remove the bio-templates. However, the etching method could reduce the shrinkage occurring in pyrolysis [25, 26].

3. Results and discussions

3.1. Microstructure of scales

Scales imbricated on the elytra of the longhorn beetle *S. mirabilis* form bright lateral stripes with a shallow greenish color as shown in the inset of figure 1(*a*). Scales are needle-like, consisting of a transparent cortex with a thickness of about 1.5 μm and an inner part with a diameter of about 8 μm.

From SEM cross-sectional images, the scale interior is an SD structure of chitin with a volume fraction about 50% [11] (figure 1(*b*)). Fourier transforms of the SEM transverse cross-sectional images of scales show that the SD structures possess only short-range order and lack well-defined local structures. Spectral measurements show that there is a broad reflection peak positioned at about 555 nm (figure 1(*c*)), leading to a shallow greenish color which is consistent with our perception.

3.2. SiO_2 SD structure

Replicated SiO_2 structures with two different methods of bio-template removal were characterized both optically and structurally as shown in figure 2. The SiO_2 structures

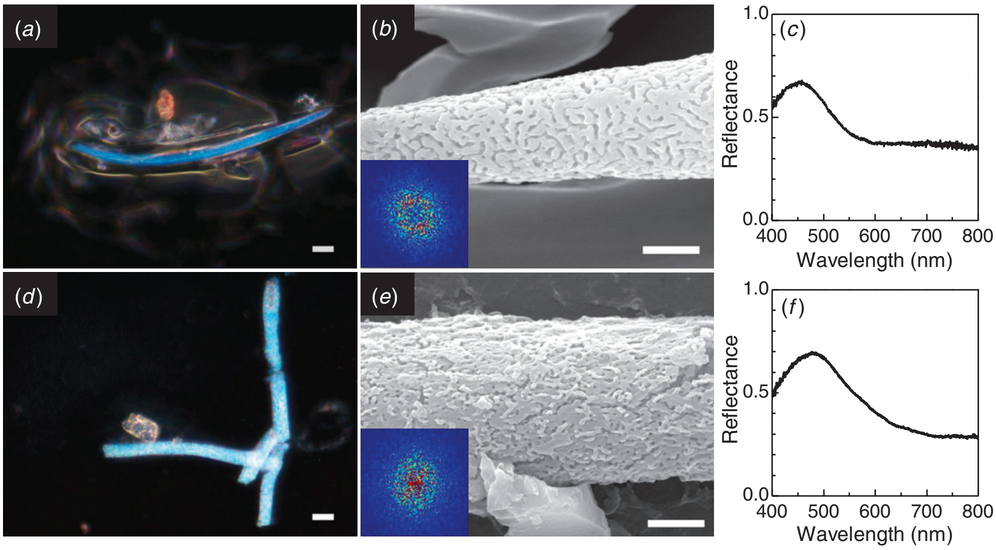

Figure 2. Optical and structural characterizations of the fabricated SiO_2 SD structures with different bio-template removal methods: pyrolysis (upper panels) and acid-etching (lower panels). (*a*) and (*d*) Optical microscopic dark-field images. Background colored stripes are produced by SiO_2 flakes on the glass slides via thin-film interference. (*b*) and (*e*) SEM images. Insets are the spectra of two-dimensional Fourier transform analysis. (*c*) and (*f*) Measured reflectance spectra. Scale bars: (*a*) and (*d*) 10 μm, and (*b*) and (*e*) 2 μm.

obtained by pyrolysis show a vivid non-iridescent blue color (figure 2(*a*)), whereas those obtained by acid-etching display a non-iridescent light blue color (figure 2(*d*)).

SEM observations indicate that the SiO_2 structures obtained by both removal methods retain the original structures of the scale interiors, i.e. SD structures, as shown in figures 2(*b*) and 2(*e*). Fourier transforms suggest that the SiO_2 SD structures possess only short-range order. Although similar in structures, the measured reflectance spectra differ in peak positions. The reflection peak is positioned respectively at 455 and 480 nm for the SiO_2 structures obtained by pyrolysis and acid-etching (figures 2(*c*) and 2(*f*)), resulting in different structural colors.

As shown in [11], SD structures can lead to structural colors owing to the existence of a photonic pseudo-gap. For an SD structure, the reflectance spectrum or perceived color depends on its characteristic length. If we keep the material refractive index unchanged and scale down the SD structure (i.e. shrinkage), its reflection peak will undergo a blue shift in wavelength. Compared with the reflection peaks of scales, the fabricated SiO_2 SD structures by both removal methods show a blue wavelength shift in reflection peak positions, implying that they all undergo a shrinkage after the post-processing of bio-template removals since the refractive index of SiO_2 ($\sim$1.5) and chitin ($\sim$1.56) is very similar. The structural quality by acid-etching is a bit poorer than that by pyrolysis. The etching method could, however, reduce the shrinkage occurring in pyrolysis since the wavelength shift of the reflection peak for acid-etching is smaller than that for pyrolysis.

3.3. TiO_2 SD structure

The high refractive index together with the large electronic band gap makes TiO_2 a promising photonic material [40] in addition to its superior photocatalytic properties [41]. TiO_2 SD structures were replicated by using an acid–base pair precursor (mixture of isopropyl titanate and $TiCl_4$). Under this condition, TiO_2 will form a crystalline anatase phase with a high refractive index of 2.5 in the visible [27]. To remove the bio-templates, the post-processing of pyrolysis was adopted.

Figure 3 shows the optical and SEM characterizations of fabricated TiO_2 SD structures. Obviously, fabricated TiO_2 SD structures show a non-iridescent blue color. Different from SiO_2 SD structures, the TiO_2 SD structures are enclosed with a thin TiO_2 layer. This is due to the shrinkage and partial recrystallization of TiO_2 during pyrolysis at high temperature. Fourier transforms indicate that the TiO_2 SD structures possess only short-range order. Spectral measurements show that there is a broad reflection peak positioned at about 445 nm due to the shrinkage and disorder of local structures.

3.4. Composition characterization

EDS measurements as shown in figure 4 were conducted to determine the chemical composition of the scales and fabricated oxide SD structures. In SiO_2 SD structures, Si and O peaks are dominant in the EDS spectra, whereas in TiO_2 SD structures Ti and O peaks dominate. The absence of C peaks in both SiO_2 and TiO_2 SD structures imply that the chitinous bio-templates were completely removed. The appearance of Au peaks is due to the sputtered gold for the sake of SEM observations. The small Si peak in the EDS spectrum of TiO_2 SD structures stems from the glass substrate.

3.5. Physical mechanism for coloration

Fabricated SiO_2 and TiO_2 SD structures display vivid non-iridescent blue colors. These colors should be structural colors resulting from the SD structures since there are no blue pigments in either fabricated or scale samples. From the Fourier transform analysis, fabricated SD structures possess

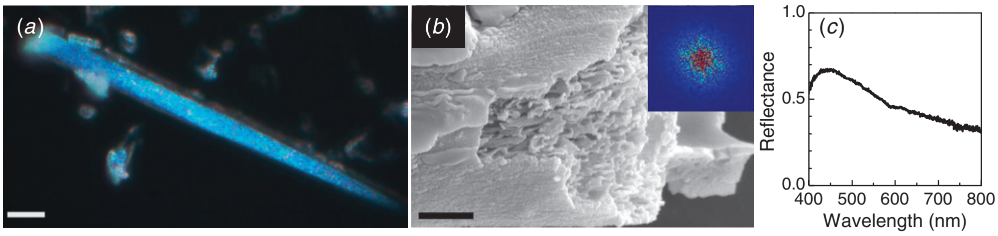

Figure 3. Optical and structural characterizations of the fabricated TiO_2 SD structures. (*a*) Optical microscopic dark-field image. (*b*) SEM image. The inset is the spectrum of two-dimensional Fourier transform analysis. (*c*) Measured reflectance spectrum. Scale bars: (*a*) 10 μm and (*b*) 2 μm.

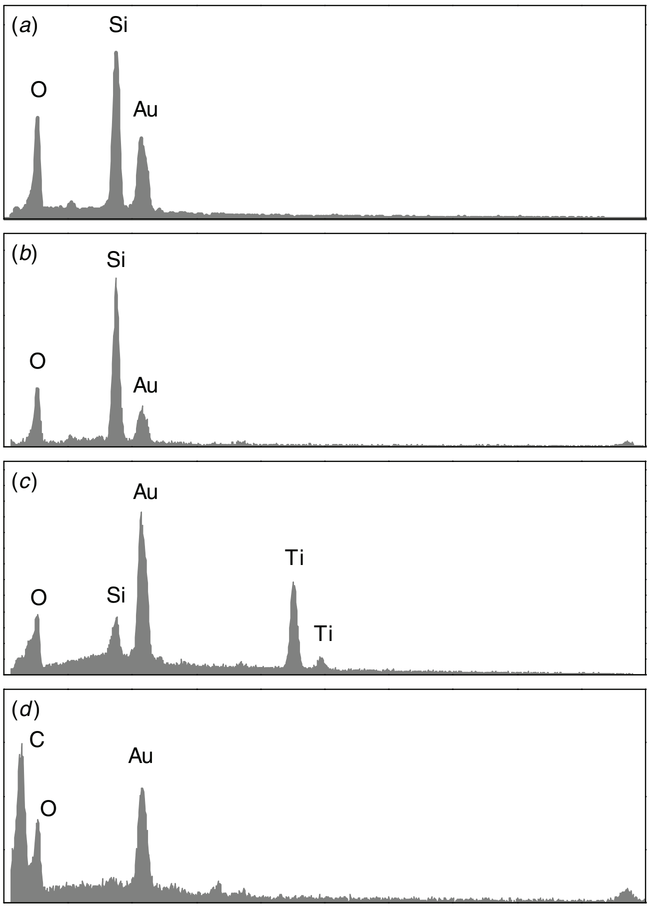

Figure 4. EDS composition analysis. (*a*) and (*b*) Spectra for SiO_2 SD structures obtained by pyrolysis and acid-etching, respectively. (*c*) Spectrum for TiO_2 SD structures. (*d*) Spectrum for scales.

only short-range order. As a result, coherent light scatterings due to the short-range order are expected [35, 37]. As shown in the simulations of photon density of states for photonic structures with only short-range order [11, 15, 38], isotropic photonic pseudo-gaps may appear. This will cause strong reflections for light frequency located within these photonic pseudo-gaps, leading to structural coloration. Non-iridescence stems from the fact that there is no preferred orientation due to lack of long-range order in SD structures.

3.6. Potential application

Different from pigment colors, structural colors are produced structurally via optical effects such as interference, diffraction, scattering or their combination [16–23]. They have many advantageous properties over pigment colors, e.g. high brightness and saturation, tunability and environmental friendliness. For photonic structures with only short-range order such as SD structures, the resulting structural colors are non-iridescent. As a result, fabricated SD structures could be exploited in color-related applications such as paint, textile and display technologies. The interesting feature of broadband reflections by SD structures makes them useful in anti-reflection coatings [42] and in solar cells as well [43, 44].

Additionally, light scattering by SD structures may have some distinct features compared with ordered photonic structures with both short- and long-range order or random structures with neither short- nor long-range order. Thus, some fundamentally interesting problems such as unusual light transport and localization [45, 46] could be studied with SD structures. With the introduction of gain materials such as laser dyes and quantum dots, random lasing may be possible [47] since light scatterings owing to the short-range order in SD structures could provide required feedbacks and amplifications.

4. Conclusions

SiO_2 and TiO_2 SD structures were successfully replicated by using a sol–gel method with the scales of the longhorn beetle *S. mirabilis* as templates. Fabricated SiO_2 and TiO_2 SD display bright non-iridescent structural colors. SEM and EDS characterizations confirm our faithful replications although there exists a shrinkage during the process of bio-template removal. Fabricated SiO_2 and TiO_2 SD structures could be potentially used in color-related applications. Owing to short-range order, they may also serve as promising candidates for studying interesting light scattering properties.

Acknowledgments

This work was supported by the 973 Program (grant nos 2013CB632701 and 2011CB922004). The research of XHL and JZ is further supported by the NSFC.

References

[1] Cahn J W 1961 On spinodal decomposition *Acta Metall.* **9** 795–801
[2] Ressine A, Ekström S, Marko-Varga G and Laurell T 2003 Macro-/nanoporous silicon as a support for

high-performance protein microarrays *Anal. Chem.* **75** 6968–74

[3] Ho C M, Yu J C, Wang X C, Lai S and Qiu Y F 2005 Meso- and macro-porous Pd/$Ce_xZr_{1-x}O_2$ as novel oxidation catalysts *J. Mater. Chem.* **15** 2193–201

[4] Ramiro-Manzano F, Atienzar P, Rodriguez I, Meseguer F, Garcia H and Corma A 2007 Apollony photonic sponge based photoelectrochemical solar cells *Chem. Commun.* 242–4

[5] Biener J, Nyce G W, Hodge A M, Biener M M, Hazma A V and Maier S A 2008 Nanoporous plasmonic metamaterials *Adv. Mater.* **20** 1211–7

[6] Vogel W 1992 *Glass Chemistry* 2nd edn (Berlin: Springer)

[7] Erlebacher J, Aziz M J, Karma A, Dimitrov N and Sieradzki K 2001 Evolution of nanoporosity in dealloying *Nature* **410** 450–3

[8] Urbas A M, Maldovan M, DeRege P and Thomas E L 2002 Bicontinuous cubic block copolymer photonic crystals *Adv. Mater.* **14** 1850–3

[9] Blin J L, Leonard A, Yuan Z Y, Gigot L, Vantomme A, Cheetham A K and Su B L 2003 Hierarchically mesoporous/macroporous metal oxides templated from polyethylene oxide surfactant assemblies *Angew. Chem. Int. Edn Engl.* **115** 2878–81

[10] Noh H, Liew S F, Saranathan V, Prum R O, Mochrie S G J, Dufresne E R and Cao H 2010 How noniridescent colors are generated by quasi-ordered structures of bird feathers *Adv. Mater.* **22** 2871–80

[11] Dong B Q, Zhan T R, Liu X H, Jiang L P, Liu F, Hu X H and Zi J 2011 Optical response of a disordered bicontinuous macroporous structure in the longhorn beetle *Sphingnotus mirabilis* *Phys. Rev.* E **84** 011915

[12] Liew S F, Yang J K, Noh H, Schreck C F, Dufresne E R, O'Hern C S and Cao H 2011 Photonic band gaps in three-dimensional network structures with short-range order *Phys. Rev.* A **84** 063818

[13] Edagawa K, Kanoko S and Notomi M 2008 Photonic amorphous diamond structure with a 3D photonic band gap *Phys. Rev. Lett.* **100** 013901

[14] Florescu M, Torquato S and Steinhardt P J 2009 Designer disordered materials with large, complete photonic band gaps *Proc. Natl Acad. Sci. USA* **106** 20658–63

[15] Yin H W, Dong B Q, Liu X H, Zhan T R, Shi L, Zi J and Yablonovitch E 2012 Amorphous diamond-structured photonic crystal in the feather barbs of the scarlet macaw *Proc. Natl Acad. Sci. USA* **109** 10798–801

[16] Fox D L 1976 *Animal Biochromes and Structural Colours* (Berkeley, CA: University of California Press)

[17] Srinivasarao M 1999 Nano-optics in the biological world: beetles, butterflies, birds and moths *Chem. Rev.* **99** 1935–61

[18] Parker A R 2000 515 million years of structural colour *J. Opt. A: Pure Appl. Opt.* **2** R15–28

[19] Vukusic P and Sambles J R 2003 Photonic structures in biology *Nature* **424** 852–5

[20] Prum R O 2006 Anatomy, physics, and evolution of avian structural colors *Bird Coloration: Mechanisms and Measurement* vol 1 ed G E Hill and K J McGraw (Cambridge, MA: Harvard University Press) pp 295–353

[21] Kinoshita S, Yoshioka S and Miyazaki J 2008 Physics of structural colors *Rep. Prog. Phys.* **71** 076401

[22] Vigneron J-P and Simonis P 2010 Structural colors *Adv. Insect Physiol.* **38** 181–218

[23] Zi J, Dong B Q, Zhan T R and Liu X H 2012 Photonic structures for coloration in the biological World *Bioinspiration: From Nano to Micro Scales* ed X Y Liu (New York: Springer) pp 275–330

[24] Parker A R 2009 Natural photonics for industrial inspiration *Phil. Trans. R. Soc.* A **364** 1759–82

[25] Galusha J W, Jorgensen M R and Bartl M H 2010 Diamond-structured titania photonic-bandgap crystals from biological templates *Adv. Mater.* **27** 107–10

[26] Galusha J W, Richey L R, Jorgensen M R, Gardner J S and Bartl M H 2010 Study of natural photonic crystals in beetle scales and their conversion into inorganic structures via a sol-gel bio-templating route *J. Mater. Chem.* **20** 1277–84

[27] Shi L, Yin H W, Zhang R Y, Liu X H, Zi J and Zhao D Y 2010 Macroporous oxide structures with short-range order and bright structural coloration: a replication from parrot feather barbs *J. Mater. Chem.* **20** 90–93

[28] Liu K and Jiang L 2011 Bio-inspired design of multiscale structures for function integration *Nano Today* **6** 155–75

[29] Biró L P and Vigneron J P 2011 Photonic nanoarchitectures in butterflies and beetles: valuable sources for bioinspiration *Laser Photon. Rev.* **5** 27–51

[30] Pulsifer D P and Lakhtakia A 2011 Background and survey of bioreplication techniques *Bioinspir. Biomim.* **6** 031001

[31] Yablonovitch E 1987 Inhibited spontaneous emission in solid-state physics and electronics *Phys. Rev. Lett.* **58** 2059–62

[32] John S 1987 Strong localization of photons in certain disordered dielectric superlattices *Phys. Rev. Lett.* **58** 2486–9

[33] Joannopoulos J D, Johnson S G, Winn J N and Meade R D 2008 *Photonic Crystals: Molding The Flow of Light* 2nd edn (Princeton, NJ: Princeton University Press)

[34] Dyck J 1971 Structure and colour-production of the blue barbs of *Agapornis roseicollis* and *Cotinga maynana* *Z. Zellforsch.* **115** 17–29

[35] Prum R O, Torres R H, Williamson S and Dyck J 1998 Coherent light scattering by blue feather barbs *Nature* **396** 28–29

[36] Shawkey M D, Estes A M, Siefferman L M and Hill G E 2003 Nanostructure predicts intraspecific variation in ultraviolet-blue plumage colour *Proc. R. Soc. Lond.* B **270** 1455–60

[37] Dufresne E R, Noh H, Saranathan V, Mochrie S G J, Cao H and Prum R O 2009 Self-assembly of amorphous biophotonic nanostructures by phase separation *Soft Matter* **5** 1792–5

[38] Dong B Q, Zhan T R, Liu X H, Jiang L P, Yin H W, Liu F and Zi J 2010 Structural coloration and photonic pseudogap in natural random close-packing photonic structures *Opt. Express* **18** 14430–8

[39] Zhang W, Zhang D, Fan T, Ding J, Guo Q and Ogawa H 2006 Morphosynthesis of hierarchical ZnO replica using butterfly wing scales as templates *Microporous Mesoporous Mater.* **92** 227–33

[40] Wijnhoven J E G J, Bechger L and Vos W L 2001 Fabrication and characterization of large macroporous photonic crystals in titania *Chem. Mater.* **13** 4486–99

[41] Linsebigler A L, Lu G Q and Yates J T 1995 Photocatalysis on TiO_2 surfaces: principles, mechanisms, and selected results *Chem. Rev.* **95** 735–58

[42] Walheim S, Schäffer E, Mlynek J and Steiner U 1999 Nanophase-separated polymer films as high-performance antireflection coatings *Science* **283** 520–2

[43] Yao Y, Hou J H, Xu Z, Li G and Yang Y 2008 Effects of solvent mixtures on the nanoscale phase separation in polymer solar cells *Adv. Funct. Mater.* **18** 1783–9

[44] Walker B, Tamayo A B, Dang X D, Zalar P, Seo J H, Garcia A, Tantiwiwat M and Nguyen T Q 2009 Nanoscale phase separation and high photovoltaic efficiency in

solution-processed, small-molecule bulk heterojunction solar cells *Adv. Funct. Mater.* **19** 3063–9

[45] John S 1984 Electromagnetic absorption in a disordered medium near a photon mobility edge *Phys. Rev. Lett.* **53** 2169–72

[46] Anderson P W 1985 The question of classical localization: a theory of white paint? *Phil. Mag.* B **52** 505–9

[47] Cao H 2003 Lasing in random media *Waves Random Media* **13** R1–39